

## STRENGTH INVESTIGATION OF TETRIX FOR THE SAFETY OF DEMONSTRATION EQUIPMENT OF AUTOMATIC CONTROL THEORY

YU YAMADA, RYOSUKE SUZUKI, TAKA AKI SUZUKI  
MASA AKI MATSUBARA AND KOU YAMADA

Graduate School of Science and Technology  
Gunma University  
1-5-1 Tenjincho, Kiryu 376-8515, Japan  
{ t161b602; r.suzuki; suzuki.taka; m.matsubara; yamada }@gunma-u.ac.jp

Received May 2017; accepted August 2017

**ABSTRACT.** *LEGO MindStorms and its expansion kit TETRIX have excellent potential to provide demonstration equipment to investigate practical effectiveness of an automatic control theory. In this paper, we investigate the strength of aluminum alloy components included in TETRIX, which LEGO company has never been released the strength data although the strength data is important for correct strength design of demonstration equipment. The tensile and bending tests were carried out to investigate the mechanical properties of the aluminum alloy components. We could obtain Young's modulus, 0.2% proof stress, ultimate tensile strength and bending strength of the aluminum alloy components. In addition, we discussed the design of the aluminum alloy component subjected to combined load of bending and torsion. Correct strength design of safety demonstration equipment for automatic control theory became possible by using strength data and technical knowledge of the component subjected to combined load.*

**Keywords:** LEGO MindStorms, TETRIX, Bending test, Strength design, Aluminum alloy

**1. Introduction.** Many kinds of machines exist in our daily experience. These machines are controlled with variety of control methods. Automatic controls provide more convenience than other control methods. Automatic controls are applied to various machines such as an air conditioner [1] to regulate the room temperature and the autopilot systems of an airplane [2]. Many theoretical and experimental studies have been performed on automatic control to develop intelligent machines and robots such as autonomous driving cars [3], automatic crane system [4], an autonomous formula racing car [5], an autonomous stair-climbing wheelchair [6] and industrial robots [7].

Demonstration equipment is required to examine practical effectiveness of an automatic control theory on an intelligent robot experimentally. However, a lot of costs, efforts and time are involved to manufacture demonstration equipment. The demonstration equipment can be manufactured inexpensively, easily and quickly by using LEGO MindStorms and expansion kit TETRIX.

LEGO MindStorms is a robot assembling kit which LEGO company started to sell in 1998. LEGO MindStorms is the teaching materials tool suitable to learn automatic controls. For example, LEGO MindStorms can provide an inverted pendulum [8] to learn automatic control theory and easy programming for the control of the pendulum. LEGO MindStorms includes a motor, a sensor, ABS resin blocks, an intelligent block and EV3 programming software. The control program can be easily created without technical knowledge of programming languages by using EV3 programming software. The created program is preserved to the intelligent block and this block is assembled into the demonstration equipment to control automatically. TETRIX includes high-strength aluminum

alloy components (U-type channel, flat bar, bracket and so on), a powerful motor and gears. Powerful demonstration equipment transporting people can be manufactured by using LEGO MindStorms and TETRIX. We should take care of safety of the demonstration equipment to prevent trouble. A designer of the demonstration equipment must adequately understand strength of the aluminum alloy components in order to assure the safety of a person on the demonstration equipment during an experiment. Correct strength design is important to manufacture the safety demonstration equipment. However, LEGO company has never released the strength data aluminum alloy components include in TETRIX required for correct design.

In this paper, we focus on the strength of aluminum alloy components included in TETRIX. The strength of the aluminum alloy components is investigated by tensile test. Bending strength of U-type channel used as beam is also investigated by three-point bending test. In addition, we discuss notice on design in the case of the U-type channel subjected to combined load of bending and torsion.

The remainder of the paper is organized as follows. In Section 2, the experimental methods are explained. In Section 3, tensile and bending strength of U-type channel are clarified and the strength of the channel subjected to combine load of bending and torsion is discussed. Section 4 concludes the paper.

## 2. Experimental Methods.

**2.1. Material.** The aluminum alloy components included in TETRIX are made of Al-Cu-Zn aluminum alloy A7005. A7000 series aluminum alloy has high strength and poor corrosion resistance. However, the aluminum alloy components also have high corrosion resistance because the surface of the components is anodized.

**2.2. Tensile test.** At first, in order to investigate the strength of the A7005 aluminum alloy components, tensile test was carried out. The specimen shown in Figure 1 was machined from a bracket. The sizes of the specimen are listed in Table 1. The tensile test was carried out under the constant cross head speed 1[mm/min]. The cross head stroke  $s$  during tensile test was measured to obtain the strain  $\varepsilon_t$ , which is calculated as next equation.

$$\varepsilon_t = \frac{s}{L_{t2}} \times 100. \quad (1)$$

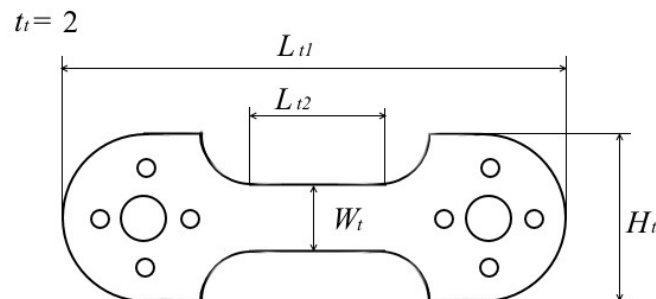


FIGURE 1. Tensile test specimen

TABLE 1. Sizes of specimen for tensile test

$L_{t1}$ [mm]	$L_{t2}$ [mm]	$H_t$ [mm]	$W_t$ [mm]	$t_t$ [mm]
91	50	27	10	2

In order to obtain Young’s modulus, the strain in the elastic region was measured by two gauge method.

**2.3. Bending test.** U-type channel (Figure 2) was used as the specimen for bending test. Schematic illustration of the specimen geometries and direction definition are shown in Figure 3 and the specimen sizes are listed in Table 2. The specimen has two kinds of holes with different diameters,  $\phi 7.9[\text{mm}]$  and  $\phi 3.7[\text{mm}]$  and these holes are regularly arranged on the specimen.

In order to clarify the bending strength of U-type channel, the three-point bending test was carried out according to ISO 7438:2005. Schematic illustration of the three point bending test is shown in Figure 4. The support span,  $L$ , is defined as next equation.

$$L = 2r_2 + 3H_s. \tag{2}$$

Here, the support radius,  $r_2 = 15[\text{mm}]$ , and the height of test piece  $H_s = 32[\text{mm}]$ . In this paper, support span  $L$  was  $126[\text{mm}]$ . Upper and lower sides of the specimen

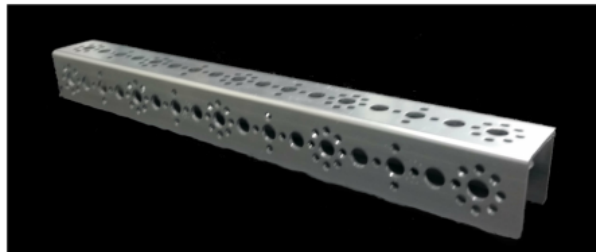


FIGURE 2. U-type channel

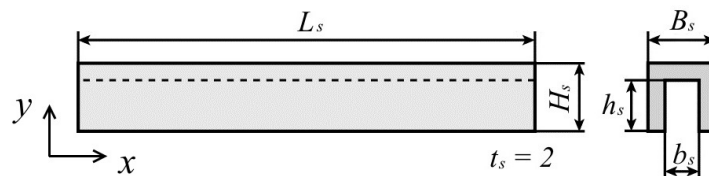


FIGURE 3. Schematic illustration of U-type channel

TABLE 2. The sizes of U-type channel

$L_s$ [mm]	$H_s$ [mm]	$B_s$ [mm]	$h_s$ [mm]	$b_s$ [mm]	$t_s$ [mm]
288	32	32	30	28	2

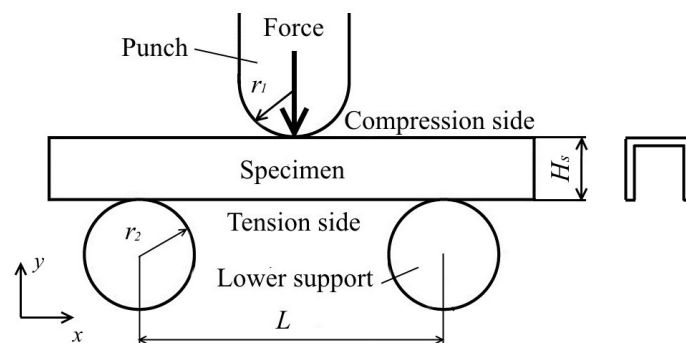


FIGURE 4. Schematic illustration of three point bending test

are subjected to compressive and tensile stresses caused by bending load, respectively. Bending test was carried out under the constant cross head speed 0.5[mm/min], and performed three times to confirm the repeatability. Maximum bending stress,  $\sigma_b$ , occurs at the center in  $x$ -direction of the specimen. Maximum bending stress is expressed as,

$$\sigma_b = \frac{M}{Z}. \quad (3)$$

Here, the bending moment,  $M$ , at the center in  $x$ -direction of the specimen is expressed as,

$$M = \frac{FL}{4}. \quad (4)$$

$F$  is bending load. The section modulus,  $Z$ , is a geometric property for given cross section area and is a function of  $y$ . The section modulus is magnitude of the resistance to bending moment, which corresponds to cross section area of a specimen to tensile load. The cross section area does not depend on the cross sectional shape; however, the section modulus depends on the cross sectional shape. Thus, the bending moment resistance of the specimens with different cross sectional shapes is different, even if the channels have the same cross section area. The both section modulus at the bottom and the upper sides of the specimen should be calculated, because the maximum tensile and compressive bending stresses occur at the bottom and the upper sides, respectively. The section modulus is expressed as,

$$Z = \frac{\int y^2 dA}{e} \quad (5)$$

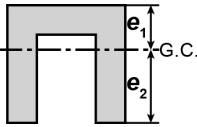
$$= \frac{I}{e} \quad (6)$$

where  $I$  is the second moment of area and  $e$  is the distance from neutral axis of the specimen to the upper or bottom side of the specimen. The second moment of area,  $I$ , is expressed as,

$$I = \frac{Be_1^3 - b_s(e_1 - t_s)^3 + 2t_s e_2^3}{3}. \quad (7)$$

$I$ ,  $e$  and  $Z$  of the specimen are listed in Table 3.

TABLE 3. Section moduli

	$e_1$ [mm]	$e_2$ [mm]	$I$ [mm <sup>4</sup> ]	$Z_{e1}$ [mm <sup>3</sup> ]	$Z_{e2}$ [mm <sup>3</sup> ]
	11.5	20.5	19707	1723	958

Bending strain  $\varepsilon_b$  of the specimen is calculated as next equation.

$$\varepsilon_b = \frac{600\delta H_s}{L^2}. \quad (8)$$

Here,  $\delta$  is the deflection of the center in  $x$ -direction of the specimen. Bending stress was plotted against bending strain and, the linear limit stress,  $\sigma_{bk}$ , 0.2% proof stress,  $\sigma_{b0.2}$  and ultimate bending stress,  $\sigma_{bu}$  were obtained.

### 3. Results and Discussion.

3.1. **Tensile test.** The tensile stress-strain curve could be obtained as shown in Figure 5. 0.2% proof stress,  $\sigma_{t0.2}$ , ultimate tensile strength,  $\sigma_{tu}$ , and Young's modulus  $E$  were obtained from Figure 5 and were listed in Table 4. These mechanical properties can be used for the design of the demonstration equipment.

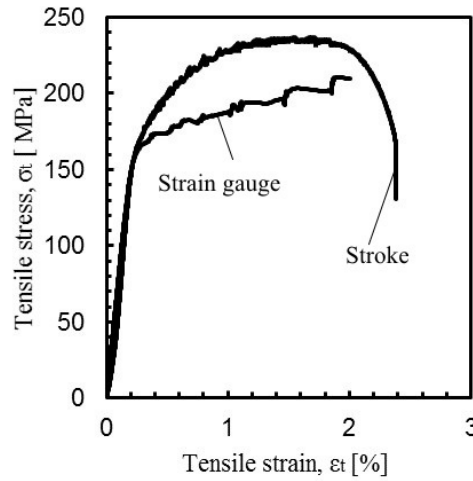


FIGURE 5. Tensile stress tensile strain curve

TABLE 4. Liner limit stress, 0.2% proof stress, ultimate bending strength and Young's modulus of aluminum alloy components

$\sigma_{tk}$ [MPa]	$\sigma_{t0.2}$ [MPa]	$\sigma_{tu}$ [MPa]	$E$ [GPa]
135	174	237	76

3.2. **Bending test.** The bending stress is plotted against the bending strain as shown in Figure 6.  $\sigma_{bk}$ ,  $\sigma_{b0.2}$ , and  $\sigma_{bu}$  were obtained from Figure 6 and were listed in Table 5. The bending strength of the U-type channel could be obtained in this paper. These parameters are very useful for correct strength design of the demonstration equipment.

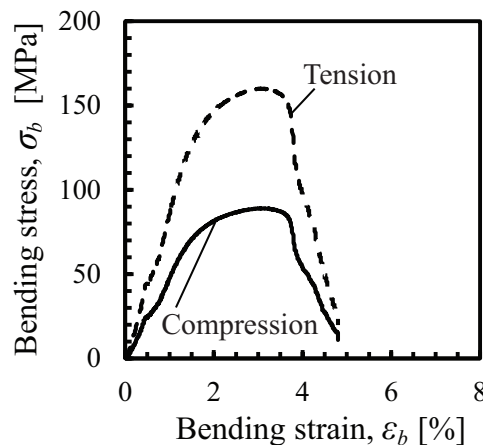


FIGURE 6. Bending stress-bending strain curve

TABLE 5. The mean liner limit stress, mean 0.2% proof stress and mean ultimate bending strength

	$\sigma_{bk}$ [MPa]	$\sigma_{b0.2}$ [MPa]	$\sigma_{bu}$ [MPa]
$e_1$	27	68	91
$e_2$	48	129	163

3.3. **Bending and torsion.** The U-type channel is subjected to combined load of the bending and torsion when the U-type channel is used such as a crane [9] and a robot arm as shown in Figure 7. The relationship between critical bending load,  $W$ , and critical torque,  $T$ , of the center of the tensile side at the yield of the U-type channel is shown as,

$$T = \frac{k_1 B_s^2 H_s}{k_2} \sqrt{\frac{1}{3} \left( \sigma_{b0.2} - \left( \frac{W}{B_s H_s^2} (H_s \sin \theta + 6b \cos \theta) \right)^2 \right)}. \tag{9}$$

Here,  $k_1$  and  $k_2$  are coefficients depending on  $B_s/H_s$ , 0.208 and 1, respectively, and  $b$  is distance between fulcrum and load.  $\theta$  is the angle between  $x$ -axis of the U-type channel and horizontal direction. The critical torque is plotted as a function of the bending load in Figure 8 at  $\theta = 0$ . The critical torque becomes low with increase of the critical bending load. Both critical bending load and torque should be considered in the design of the demonstration equipment when the U-type channel is subjected to combined load of the bending and torsion. In addition, the critical torque at the center of the side parallel to  $y$ -direction should be considered in the strength design for the safety of demonstration equipment because the maximum share stress occurs at this position by applied torque.

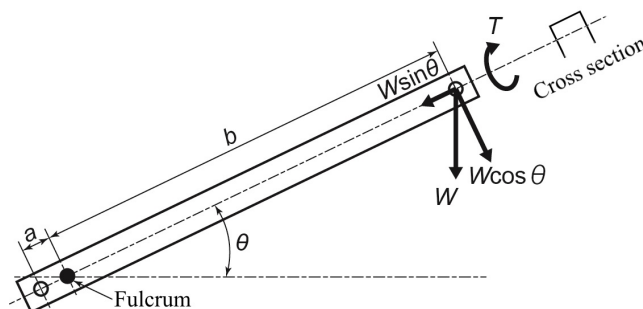


FIGURE 7. Problem of crane

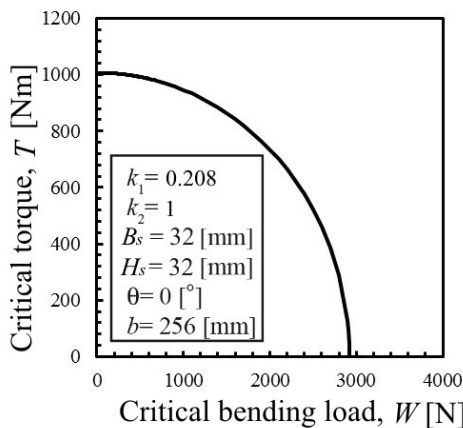


FIGURE 8. Critical bending and torque

**4. Conclusions.** The mechanical properties of aluminum alloy components included in TETRIX have ever been released by LEGO company, although these data are important to assure the safety of a person on the demonstration equipment made of TETRIX during an experiment. In this paper, the mechanical properties of the aluminum alloy components were clarified. In addition, we discussed relationship between critical bending load and critical torque when the U-type channel is subjected to combined load of the bending and torsion. As a result, we can design and manufacture safety demonstration equipment for automatic control theory by using the mechanical properties of TETRIX and technical knowledge of combined load of bending and torque obtained by this paper. In the future, we construct a useful automatic control theory to the demonstration equipment which can carry a person and a load at first. And we design and manufacture the secure demonstration equipment made from TETRIX using the strength data obtained in this paper. We carry out demonstration of new theory safely using the demonstration equipment.

#### REFERENCES

- [1] W. Viriyautsahakul, W. Panacharoenwong, W. Pongpiriyakijkul, S. Kosolsaksakul and W. Nakawiro, A simulation study of inverter air conditioner controlled to supply reactive power, *Procedia Computer Science*, vol.86, pp.305-308, 2016.
- [2] J. Weyer, Confidence in hybrid collaboration. An empirical investigation of pilots' attitudes towards advanced automated aircraft, *Safety Science*, vol.89, pp.167-179, 2016.
- [3] E. Drozdova, S. Hopfgarten, E. Lazutkin and P. Li, Autonomous driving of a mobile robot using a combined multiple-shooting and collocation method, *The 9th IFAC Symposium on Intelligent Autonomous Vehicles IAV 2016*, vol.49, pp.193-198, 2016.
- [4] N. Boysen and K. Stephan, A survey on single crane scheduling in automated storage/retrieval systems, *European Journal of Operational Research*, vol.254, pp.691-704, 2016.
- [5] J. Ni and J. Hu, Dynamics control of autonomous vehicle at driving limits and experiment on an autonomous formula racing car, *Mechanical Systems and Signal Processing*, vol.90, pp.154-174, 2017.
- [6] M. Hinderer, P. Friedrich and B. Wolf, An autonomous stair-climbing wheelchair, *Robotics and Autonomous Systems*, vol.94, pp.219-225, 2017.
- [7] F. Leutert and K. Schilling, Augmented reality for telemaintenance and -inspection in force-sensitive industrial robot applications, *The 2nd IFAC Conference on Embedded Systems, Computer Intelligence and Telematics*, vol.48, pp.153-158, 2015.
- [8] R. E. Seifullaev, Speed gradient energy and sampled-data control of cart-pendulum system, *The 9th IFAC Symposium Advances in Control Education*, vol.45, pp.478-483, 2012.
- [9] Y. Fang, Y. Cho and J. Chen, A framework for real-time pro-active safety assistance for mobile crane lifting operations, *Automation in Construction*, vol.72, pp.367-379, 2016.